NASA TECHNICAL MEMORANDUM

NASA TM X-2840

NASA TM X-2840

STARTUP ANALYSIS FOR A HIGH-TEMPERATURE GAS-LOADED HEAT PIPE

by Peter M. Sockol

Lewis Research Center

Cleveland, Ohio 44135

NATIONAL AERONAUTICS AND SPACE ADMINISTRATION • WASHINGTON, D. C. • JULY 1973

1. Report No.	2. Government Accession No.	3. Recipient's Catalog No.
NASA TM X-2840		

4. Title and Subtitle	5. Report Date
STARTUP ANALYSIS FOR A HIGH-TEMPERATURE GAS-LOADED HEAT PIPE	July 1973
	6. Performing Organization Code

7. Author(s)	8. Performing Organization Report No.
Peter M. Sockol	E-7416
	10. Work Unit No. 503-25

9. Performing Organization Name and Address	11. Contract or Grant No.
Lewis Research Center National Aeronautics and Space Administration Cleveland, Ohio 44135	

12. Sponsoring Agency Name and Address	13. Type of Report and Period Covered
National Aeronautics and Space Administration Washington, D.C. 20546	Technical Memorandum
	14. Sponsoring Agency Code

15. Supplementary Notes

16. Abstract

A model for the rapid startup of a high-temperature gas-loaded heat pipe is presented. A two-dimensional diffusion analysis is used to determine the rate of energy transport by the vapor between the hot and cold zones of the pipe. The vapor transport rate is then incorporated in a simple thermal model of the startup of a radiation-cooled heat pipe. Numerical results for an argon-lithium system show that radial diffusion to the cold wall can produce large vapor flow rates during a rapid startup. The results also show that startup is not initiated until the vapor pressure p_v in the hot zone reaches a precise value proportional to the initial gas pressure p_i. Through proper choice of p_i, startup can be delayed until p_v is large enough to support a heat-transfer rate sufficient to overcome a thermal load on the heat pipe.

17. Key Words (Suggested by Author(s))	18. Distribution Statement
Heat pipes Gas-loaded heat pipes Heat transfer	Unclassified - unlimited

19. Security Classif. (of this report)	20. Security Classif. (of this page)	21. No. of Pages	22. Price*
Unclassified	Unclassified	19	$3.00

* For sale by the National Technical Information Service, Springfield, Virginia 22151

STARTUP ANALYSIS FOR A HIGH-TEMPERATURE GAS-LOADED HEAT PIPE

by Peter M. Sockol

Lewis Research Center

SUMMARY

A model for the rapid startup of a high-temperature gas-loaded heat pipe is presented. A two-dimensional diffusion analysis is used to determine the rate of energy transport by the vapor between the hot and cold zones of the pipe. The vapor transport rate is then incorporated in a simple thermal model of the startup of a radiation-cooled heat pipe. Numerical results for an argon-lithium system show that radial diffusion to the cold wall can produce large vapor flow rates during a rapid startup. The results also show that startup is not initiated until the vapor pressure p_v in the hot zone reaches a precise value proportional to the initial gas pressure p_i. Through proper choice of p_i, startup can be delayed until p_v is large enough to support a heat-transfer rate sufficient to overcome a thermal load on the heat pipe.

INTRODUCTION

A gas-loaded heat pipe contains a fixed quantity of a noncondensible gas in addition to its working fluid. The introduction of a gas into an ordinary heat pipe has been suggested as a means of aiding its startup. When a high-temperature heat pipe is closely coupled to a thermal sink, the very low initial vapor pressure may make it incapable of delivering the energy demanded during startup (ref. 1). Some technique must be found to decrease the coupling between the pipe and the sink if startup is to be successful.

During operation of a gas-loaded heat pipe, vapor flows from the evaporator to the condensor and the noncondensible gas is carried with it. The gas collects in the end of the condensor and decreases the effective heat-rejection area. As the temperature, and hence the vapor pressure, in the evaporator is increased, the gas is compressed to a smaller volume. If a sufficient quantity of gas is introduced, the heat pipe can be completely decoupled from the thermal sink until the vapor pressure is high enough to support large energy transport rates.

Before a gas-loaded heat pipe is incorporated in a larger system it is necessary to be able to predict its performance during startup. To this end a two-dimensional analysis of the diffusion of vapor through the gas in the condensor is performed in the present work. The energy transport rate obtained in this study is combined with a simple thermal model of the startup of a radiation-cooled heat pipe. Numerical results are presented for a long lithium heat pipe with argon as the noncondensible gas. They should be of value in the design of experiments with high temperature gas-loaded heat pipes.

SYMBOLS

A_i	expansion coefficient, eq. (18)
A_r	parameter, eq. (31)
A_v	parameter, eq. (32)
a_i	expansion coefficient, eq. (23)
B_i	expansion coefficient, eq. (19)
b_i	expansion coefficient, eq. (24)
C	heat capacity per unit length
c	total molar density
c_i	initial molar concentration of noncondensible gas
D	outside diameter of heat pipe
D_θ	parameter, eq. (36)
D_ℓ	parameter, eq. (37)
$\mathscr{D}$	binary diffusion coefficient
E_1	exponential integral
$F_c(g)$	function, eq. (16)
$F_h(g)$	function, eq. (17)
g	dimensionless vapor flux
h_{fg}	heat of vaporization per unit mass
J_o	Bessel function
L	length of hot zone
L_e	length of evaporator

L_p length of heat pipe

ℓ dimensionless L

ℓ_e dimensionless L_e

ℓ_p dimensionless L_p

M_v molecular weight of vapor

N_o vapor flux, eq. (3)

$\bar{N}_v$ molar vapor flux

p_i initial pressure of noncondensible gas

$p_v(T)$ vapor pressure

Q heat input

Q_r heat lost by radiation

Q_v energy transported by vapor

q dimensionless Q

q_r dimensionless Q_r

q_v dimensionless Q_v

R radius

R_w inside radius of wick

r dimensionless R

T temperature of hot zone

T_c temperature of cold zone

t time

t_i time at which Q is switched on

x_g mole fraction of noncondensible gas

x_v mole fraction of vapor

y concentration variable, eq. (9)

Z distance along pipe

z dimensionless Z

α_i zeros of J_o'

β_i zeros of J_o

γ Euler constant

δ_{ij} Kronecker delta, eq. (20)

ϵ emissivity of pipe wall

θ dimensionless T

$\lambda(\theta, l)$ function, eq. (8)

λ_θ parameter, eq. (33)

σ Stefan-Boltzmann constant

Subscripts:

c cold zone

h hot zone

Superscript:

$( )'$ differentiation with respect to argument

DESCRIPTION OF THE MODEL AND ASSUMPTIONS

Thermal Model

The thermal model has already been applied to the startup of an ordinary radiation-cooled heat pipe (refs. 2 and 3). When the power is turned on, a hot zone of uniform wall temperature T forms in the evaporator. Once the vapor pressure $p_v(T)$ is high enough, the front edge of this zone begins to move into the condensor. Despite the steep wall-temperature gradient at the front, it is assumed that axial heat conduction in the wall is negligible compared to energy transport by vapor diffusion. The remaining cold zone retains its initial temperature T_c.

This model is in definite opposition to the results of the steady-state analysis of reference 4. There it is shown that at the front axial heat conduction in the wall is much greater than energy transport by the diffusing vapor. The present calculations confirm that the vapor flow rate past the front becomes quite small as steady state is approached. They also show, however, that very large diffusion rates accompany the motion of the temperature front during startup. Such rates are incompatible with a stationary front.

Diffusion Model

The goal of the diffusion analysis is to determine the vapor flow rate past the temperature front as a function of the length and temperature of the hot zone. To simplify

the calculations the local condensation rate upstream of the front is assumed to be negligible, whereas the cold wall is taken to act as a perfect sink for the vapor. The transition region between these two boundary conditions is considered to be vanishingly thin. The nonuniform vapor velocity in the hot zone must produce a secondary flow of noncondensible gas. This effect is neglected, however; the upstream velocity is assumed uniform over the cross section, and the gas is taken to be stagnant throughout the pipe. The axial pressure drop is neglected, and the total pressure, gas plus vapor, is set equal to the vapor pressure $p_v(T)$ in the evaporator. This restricts the analysis to cases where the vapor velocity is much less than the speed of sound during startup. In a long cylindrical heat pipe the vapor concentration should relax to a quasi-steady profile in a time of order $(R_w/2.4)^2/\mathscr{D}$, where R_w is the inside radius of the wick and $\mathscr{D}$ is the binary diffusion coefficient for the vapor-gas mixture. If the distance moved by the temperature front during this time is small, then steady-flow equations can be used in the diffusion analysis. In an argon-lithium heat pipe at 1300 K, with $R_w = 1$ centimeter, the relaxation time is about 10 milliseconds. For a typical case (fig. 3) the maximum frontal motion during this time is 0.02 centimeter which is small. Finally, the product $c\mathscr{D}$, where c is the total molar density, is assumed constant and evaluated at the average of the temperatures T and T_c.

DIFFUSION ANALYSIS

The molar flux of vapor N_v through a stagnant gas is given by (ref. 5)

$$\vec{N}_v = x_v \vec{N}_v - c\mathscr{D} \vec{\nabla} x_v = c\mathscr{D} \vec{\nabla} \ln x_g \tag{1}$$

where x_v and x_g are the mole fractions of vapor and gas, respectively. Conservation of mass requires

$$\nabla^2 \ln x_g = 0 \tag{2}$$

A cylindrical coordinate system is introduced with the main flow in the Z direction and the origin at the interface between the hot and cold zones (fig. 1). It is assumed that the axial distance over which x_g departs significantly from 0 or 1 is small compared to L or $L_p - L$ where L is the length of the hot zone and L_p is the length of the heat pipe. Hence, the boundaries on equation (2) are taken at $Z = \pm\infty$. The boundary conditions for equation (2) are as follows:

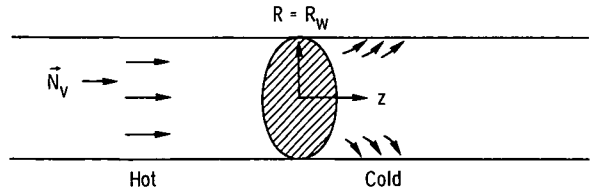

Figure 1. - Coordinate system for diffusion analysis with main flow in Z-direction and origin at interface between hot and cold zones.

For $Z < 0$:

$$c\mathscr{D}\frac{\partial}{\partial Z}\ln x_g \to N_o \qquad \text{as} \quad Z \to -\infty \tag{3}$$

$$\frac{\partial}{\partial R}\ln x_g = 0 \qquad \text{at} \quad R = R_w \tag{4}$$

For $Z > 0$:

$$x_g \to 1 \qquad \text{as} \quad Z \to \infty \tag{5}$$

$$x_g = 1 \qquad \text{at} \quad R = R_w \tag{6}$$

where N_o is an unknown constant flux. Conditions (4) and (6) represent no condensation and the perfect sink, respectively. The unknown N_o is determined by specifying the initial molar concentration c_i of the noncondensible gas at temperature T_c. A mass balance on the gas gives

$$c_i L_p = \int_{-L}^{L_p - L} \overline{cx_g}\, dZ \approx \int_{-\infty}^{0} \overline{cx_g}\, dZ + \int_{0}^{\infty} \overline{c(x_g - 1)}dZ + \int_{0}^{L_p - L} c\, dZ$$

$$\approx c_h \int_{-\infty}^{0} \overline{x_g}\, dZ - c_c \int_{0}^{\infty} \overline{(1 - x_g)}dZ + c_c(L_p - L) \tag{7}$$

where the bar indicates an average over the cross section, and c_h and c_c are constants obtained by evaluating c at the temperatures T and T_c, respectively. Note that the integrands in equation (7), as finally written, go rapidly to zero away from $Z = 0$.

Dimensionless variables are introduced:

$$r = \frac{R}{R_w}, \qquad z = \frac{Z}{R_w}, \qquad g = \frac{N_o R_w}{c\mathscr{D}}$$

$$\ell = \frac{L}{R_w}, \qquad \ell_p = \frac{L_p}{R_w}, \qquad \theta = \frac{T}{T_c}$$

and

$$\lambda(\theta, \ell) = \frac{\left[c_c(L_p - L) - c_i L_p\right]}{c_c R_w} = \ell_p - \ell - \frac{\ell_p p_i}{p_v(T)} \tag{8}$$

where p_i is the initial gas pressure. A new dependent variable y is defined by

$$\ln x_g = -gy \tag{9}$$

In cylindrical coordinates, equation (2) becomes

$$\frac{1}{r}\frac{\partial}{\partial r}\left(r\,\frac{\partial y}{\partial r}\right) + \frac{\partial^2 y}{\partial z^2} = 0 \tag{10}$$

Equations (3) to (6) become the following:

For $z < 0$:

$$\frac{\partial y}{\partial z} \to -1 \qquad \text{as} \quad z \to -\infty \tag{11}$$

$$\frac{\partial y}{\partial r} = 0 \qquad \text{at} \quad r = 1 \tag{12}$$

For $z > 0$:

$$y \to 0 \qquad \text{as} \quad z \to \infty \tag{13}$$

$$y = 0 \qquad \text{at} \quad r = 1 \tag{14}$$

Equation (7) becomes

$$F_c(g) - \theta^{-1} F_h(g) = \lambda(\theta, l) \tag{15}$$

with

$$F_c(g) = 2 \int_0^1 r\, dr \int_0^\infty (1 - e^{-gy}) dz \tag{16}$$

$$F_h(g) = 2 \int_0^1 r\, dr \int_{-\infty}^0 e^{-gy}\, dz \tag{17}$$

Once $y(r, z)$ is determined, equation (15) can be solved numerically to obtain g, and hence the mass flux as a function of T and l.

The solution of equations (10) to (14) is given by the following:

$z < 0$:

$$y = -z + \sum_{i=1}^{\infty} A_i e^{\alpha_i z} J_o(\alpha_i r), \qquad J_o'(\alpha_i) = 0 \tag{18}$$

$z > 0$:

$$y = \sum_{i=1}^{\infty} B_i e^{-\beta_i z} J_o(\beta_i r), \qquad J_o(\beta_i) = 0 \tag{19}$$

Note that $\alpha_1 = 0$ and $J_o(0) = 1$. The Bessel functions $J_o(\alpha_i r)$ and $J_o(\beta_i r)$ satisfy the following relations (ref. 6, ch. 11):

$$2 \int_0^1 r J_o(\alpha_i r) J_o(\alpha_j r) dr = \delta_{ij} \left[J_o(\alpha_j)\right]^2 \tag{20}$$

$$2 \int_0^1 r J_o(\beta_i r) J_o(\beta_j r) dr = \delta_{ij} \left[J_o'(\beta_j)\right]^2 \tag{21}$$

$$2 \int_0^1 r J_o(\alpha_i r) J_o(\beta_j r) dr = 2\beta_j \left(\alpha_i^2 - \beta_j^2\right)^{-1} J_o(\alpha_i) J_o'(\beta_j) \tag{22}$$

where $\delta_{ii} = 1$ and $\delta_{ij} = 0$ for $i \neq j$. Requiring y and $\partial y/\partial z$ to be continuous at $z = 0$ and applying relations (18) to (20) to the results give

$$a_j = -2\sum_{i=1}^{\infty} b_i\beta_i\left(\alpha_j^2 - \beta_i^2\right)^{-1}, \qquad j = 1, \ldots, \infty \tag{23}$$

$$b_j = 2\sum_{i=1}^{\infty} a_i\alpha_i\left(\alpha_i^2 - \beta_j^2\right)^{-1} + 2\beta_j^{-2}, \qquad j = 1, \ldots, \infty \tag{24}$$

where $a_i = A_iJ_0(\alpha_i)$ and $b_i = -B_iJ_0'(\beta_i)$. A finite subset of equations (23) and (24) with $j = 1, \ldots, n$ can be solved by iteration. Final values are obtained by increasing n until the low order coefficients no longer change. For $n = 30$ the first few coefficients are

$a_1 = 0.2537$	$b_1 = 0.2578$
$a_2 = -0.0761$	$b_2 = 0.0638$
$a_3 = -0.0336$	$b_3 = 0.0308$
$a_4 = -0.0201$	$b_4 = 0.0188$
$a_5 = -0.0138$	$b_5 = 0.0129$

The remaining coefficients decrease quite slowly, but the exponential factors in equations (16) and (17) ensure adequate convergence away from $z = 0$.

Once g has been found by solving equation (15), the energy transport by diffusion from the hot to the cold zone Q_v is given by

$$Q_v = \pi R_w^2 M_v N_0 h_{fg} = \pi R_w M_v c\mathscr{D} h_{fg} g \tag{25}$$

where M_v is the molecular weight of the vapor and h_{fg} is its heat of vaporization per unit mass. For g of order one this corresponds to a very small energy transport. As an example, in an argon-lithium heat pipe at 1300 K with $R_w = 1$ centimeter and $g = 1$, equation (25) gives $Q_v \approx 7.4$ watts. For large transport rates to occur it is therefore necessary to have $g \gg 1$. From equations (9) and (19) this corresponds to the bulk of the gas being pushed far enough into the cold zone to enable the vapor to reach the cold surface by diffusing radially through a very thin layer of gas.

The functions $F_c(g)$ and $F_h(g)$ must be evaluated numerically. The results have been approximated by analytical expressions for subsequent use. For $g \gg 1$, however, F_c is dominant and the following approximation is of interest. If only the first term in

the series of equation (19) is retained, equation (16) gives

$$F_c(g) \approx 2 \int_0^1 r\,dr \int_0^\infty \left\{1 - \exp\left[-gB_1 J_o(\beta_1 r) e^{-\beta_1 z}\right]\right\} dz$$

$$\approx 2 \int_0^1 r\,dr\, \beta_1^{-1} \int_0^{gB_1 J_o(\beta_1 r)} (1 - e^{-t}) \frac{dt}{t}$$

$$\approx 2 \int_0^1 r\,dr\, \beta_1^{-1} \left\{\gamma + \ln\left[gB_1 J_o(\beta_1 r)\right] + E_1\left[gB_1 J_o(\beta_1 r)\right]\right\}$$

$$\approx \beta_1^{-1} (\ln g - 1.339) \qquad (26)$$

where $\gamma = 0.5772$. The radial integral was performed numerically. Note that the exponential integral (ref. 6, ch. 3) $E_1(x)$ approaches zero for large x. Hence, $F_c(g)$ has only a weak dependence on g for $g \gg 1$.

TIME-DEPENDENT THERMAL ANALYSIS

The time-dependent equations are written for a radiation-cooled heat pipe with a shielded evaporator. The state of the heat pipe at time t is shown in figure 2, where Q is the heat input to the evaporator, Q_r the heat lost by radiation, and Q_v the energy transported by the vapor to the cold zone.

When the hot zone is expanding into the condensor, energy balances on control vol-

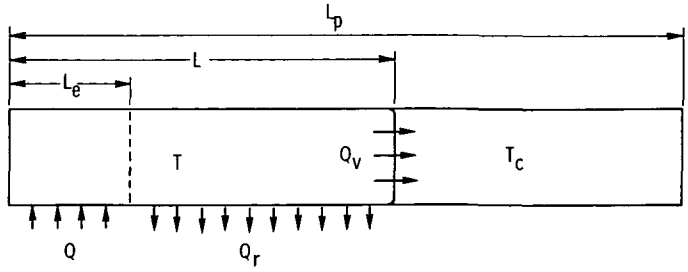

Figure 2. - State of heat pipe at time t.

umes enclosing the hot and cold zones, respectively, at time t give

$$CL \frac{dT}{dt} = Q - Q_r - Q_v \tag{27}$$

$$C(T - T_c) \frac{dL}{dt} = Q_v \tag{28}$$

where C is the heat capacity per unit length of the wall, wick, and liquid. In terms of θ and l these equations become

$$l \frac{d\theta}{dt} = q - q_r - q_v \tag{29}$$

$$(\theta - 1) \frac{dl}{dt} = q_v \tag{30}$$

with $q = Q/CR_wT_c$. The quantities q_r and q_v are given by

$$q_r = A_r \theta^4 (l - l_e) \tag{31}$$

$$q_v = A_v g \tag{32}$$

where $A_r = \pi D \epsilon \sigma T_c^3/C$, $l_e = L_e/R_w$, and $A_v = \pi M_v (c\mathscr{D}) h_{fg}/CT_c$. Also, D is the outside diameter of the pipe, ϵ the emissivity, and σ the Stefan-Boltzmann constant. The formulation is completed by equation (15) with $\lambda(\theta, l)$ given by equation (8).

During the initial startup period, q_v remains negligibly small until $p_v(T) > p_i$ and $\lambda > 0$. For $\lambda > 0$, there is an extremely rapid transient in which q_v approaches q and $d\theta/dt$ becomes small. Thereafter, both l and θ increase at moderate rates, and q_v decreases steadily as q_r increases. This continues until steady state is approached. The behavior is illustrated in figure 3 for an argon-lithium heat pipe.

In this latter period, equation (15) causes a severe numerical difficulty. The function $\lambda(\theta, l)$ has a very strong dependence on θ and l, while $F_c(g)$ is a weak function of g for $g \gg 1$. Thus, q_v is extremely sensitive to small changes in θ and l, which makes equations (29) and (30) numerically unstable for any reasonable size integration step (>0.1 sec).

Since $l(d\theta/dt)$ is small compared to $(q - q_r)$ in this period, equation (29) can be used to obtain an approximate value of q_v and hence g. Equations (30) and (15) can then be solved simultaneously for l and θ. It is necessary, however, to first obtain a good ap-

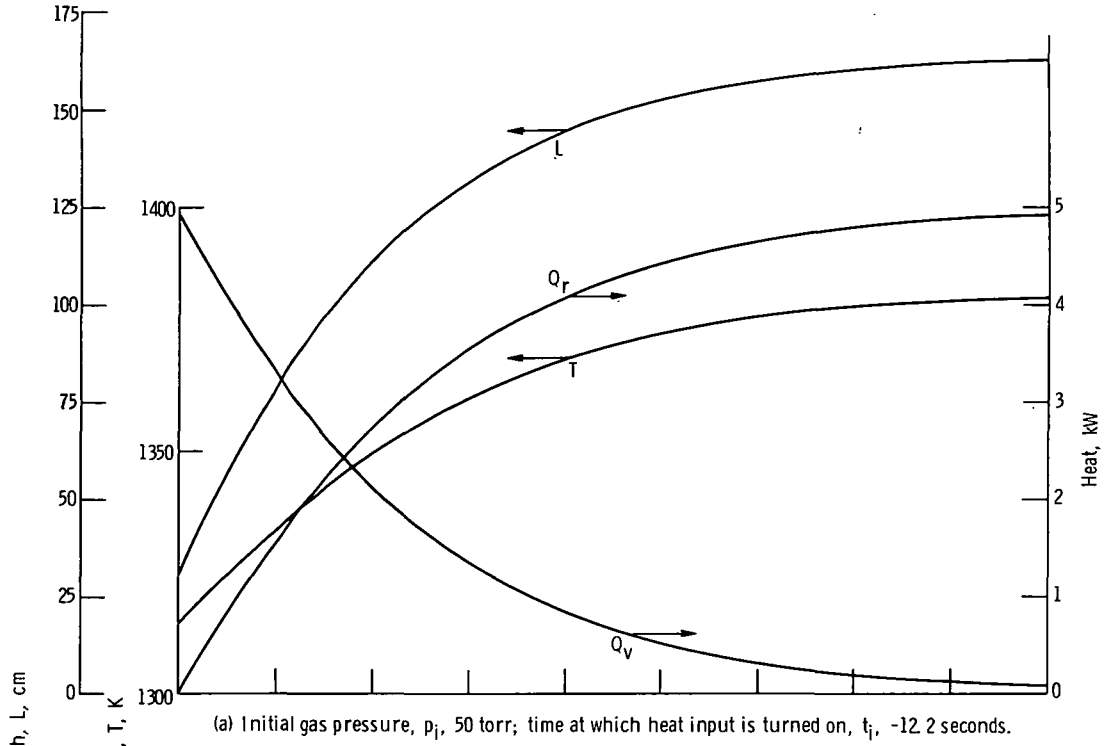

(a) Initial gas pressure, p_i, 50 torr; time at which heat input is turned on, t_i, -12.2 seconds.

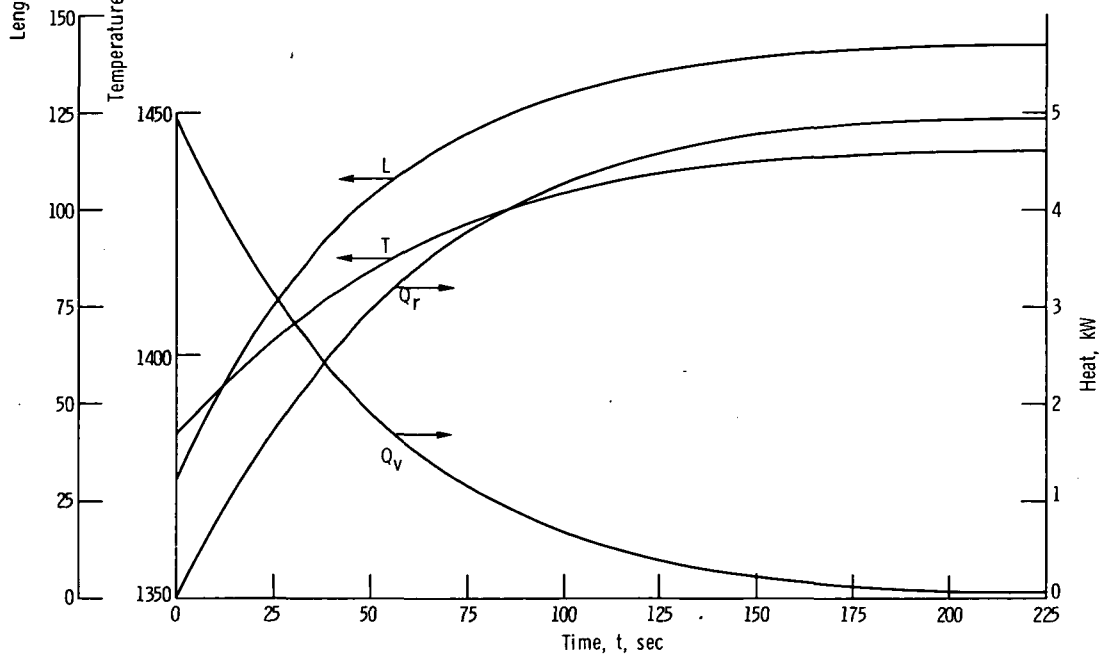

(b) Initial gas pressure, p_i, 100 torr; time at which heat input is turned on, t_i, -13.0 seconds.

Figure 3. - Startup behavior for argon-lithium heat pipe with constant heat input. Length of heat pipe, L_p, 300 centimeters; length of evaporator, L_e, 30 centimeters; heat input, Q, 5 kilowatts.

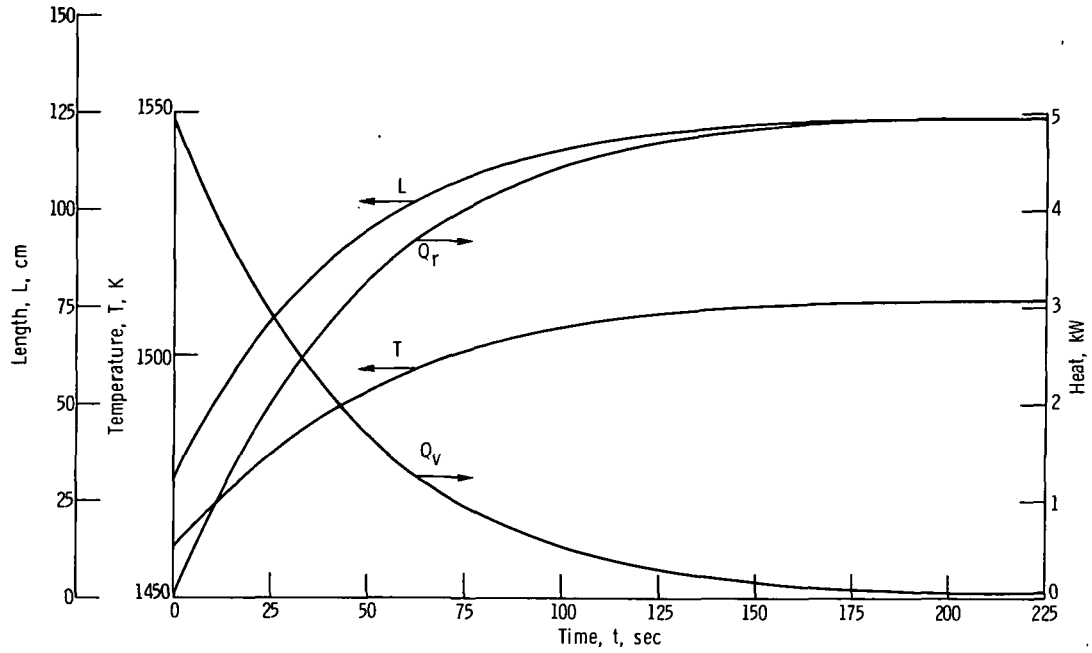

(c) Initial gas pressure, p_i, 200 torr; time at which heat input is turned on, t_i, -13.9 seconds.

Figure 3. - Concluded.

proximation to $d\theta/dt$. Differentiating equations (15) and (8) gives

$$\left[\lambda_e - \theta^{-2} F_h(g)\right] \frac{d\theta}{dt} - \frac{dl}{dt} = \left[F_c'(g) - \theta^{-1} F_h'(g)\right] \frac{dg}{dt} \tag{33}$$

with $\lambda_\theta = T_c l_p p_i p_v'/p_v^2$. Equation (29), with $l(d\theta/dt)$ assumed small and q taken as constant, gives

$$\frac{dg}{dt} \approx -\frac{A_r}{A_v}\left[4\theta^3 (l - l_e)\frac{d\theta}{dt} + \theta^4 \frac{dl}{dt}\right] \tag{34}$$

Equations (33) and (34) give

$$D_\theta \frac{d\theta}{dt} - D_l \frac{dl}{dt} \approx 0 \tag{35}$$

with

$$D_\theta = \lambda_\theta - \theta^{-2} F_h + \left(F_c' - \theta^{-1} F_h'\right)\frac{A_r}{A_v} \cdot 4\theta^3 (l - l_e) \tag{36}$$

$$D_l = 1 - \left(F_c' - \theta^{-1} F_h'\right) \frac{A_r}{A_v} \theta^4 \tag{37}$$

Equations (29), (30), and (35) give

$$\left[l + (\theta - 1) \frac{D_\theta}{D_l} \right] \frac{d\theta}{dt} \approx q - q_r \tag{38}$$

Finally, equations (29) and (38) give

$$q_v \approx (q - q_r) \frac{(\theta - 1) D_\theta}{(\theta - 1) D_\theta + l D_l} \tag{39}$$

Equations (30), (15), and (39) form a system of one differential and two algebraic equations whose solution approximates that of equations (29), (30), and (15) when $d\theta/dt$ is small. The stability of this approximate set of equations is much improved over that of the original set.

Both sets of equations have been incorporated in a numerical integration scheme. The initial conditions at $t = 0$ are taken to be $l_o = l_e$ and $\lambda(\theta_o, l_o) = 0$. From equation (8) this gives

$$p_v(T_o) = \frac{p_i l_p}{(l_p - l_e)} \tag{40}$$

At earlier times $q_r = 0$, $q_v \approx 0$, and $\theta = 1 + q(t - t_i)/l_e$ where t_i is the time when Q is switched on. The integration is started using the original set of equations and a very small integration step. When q_v is close to its maximum value, the integration is continued using the approximate equations. The numerical routine automatically varies the size of the integration step to achieve the maximum value consistent with accuracy and stability. In a typical case the stepsize varied from 10^{-4} second at the start to 10 seconds at the end of the integration. In a few cases the approximation was checked by using the original set of equations throughout the calculation. The agreement between the two methods was better than three significant figures in l and θ. Solutions have also been obtained for a startup in which Q is increased in steps until the final steady state is reached.

NUMERICAL RESULTS

The time-dependent theory of the preceding section has been applied to the startup of an argon-lithium heat pipe. The specifications of the pipe are as follows: L_p = 300 centimeters, L_e = 30 centimeters, D = 1.9 centimeters, R_w = 0.78 centimeter, C = 1.99 joules per centimeter per degrees Kelvin, and ϵ = 0.3. The values for R_w, C, and ϵ were obtained by selecting a 1.0 millimeter thick tantalum alloy wall, an 0.5-millimeter-thick annular liquid return, and an 0.2-millimeter-thick tungsten screen wick with 50-percent porosity. The binary diffusion coefficient was evaluated from the Chapman-Enskog expression (ref. 7) with measured values of the Lennard-Jones parameters for the argon-lithium interaction (ref. 8).

Figure 3 shows the results for startup with a constant heat input Q of 5 kilowatts and initial gas pressures p_i of 50, 100, and 200 torr. The switch on times t_i for these cases are -12.2, -13.0, and -13.9 seconds, respectively. At t = 0 the vapor energy transport Q_v increases from near zero to slightly less than Q in less than 0.02 second. In this period of time the vapor pressure $p_v(T)$ increased by only 0.7 percent, but this is sufficient to raise the parameter λ (eq. (8)) from 0 to 2.2. It should be noted that it takes about the same length of time to establish a steady-state concentration profile in an argon-lithium system of the previously given dimensions at these pressures and temperatures. Nevertheless, the figures show that in each case startup is initiated at a very precise temperature T_o given by equation (36). This fact can be used to eliminate startup difficulties in many applications. Since the heat-transfer capability of the heat pipe increases with the vapor pressure p_v, the initial gas pressure p_i can be increased to the point where startup is not initiated until p_v is large enough to support a heat-transfer rate large enough to overcome the thermal load on the condensor.

Figure 4 shows the results for a startup in which Q is increased in steps to 25 kilowatts with p_i = 50 torr. In this way the vapor flow rate at the evaporator exit does not reach a very large value until p_v is large enough to sustain it.

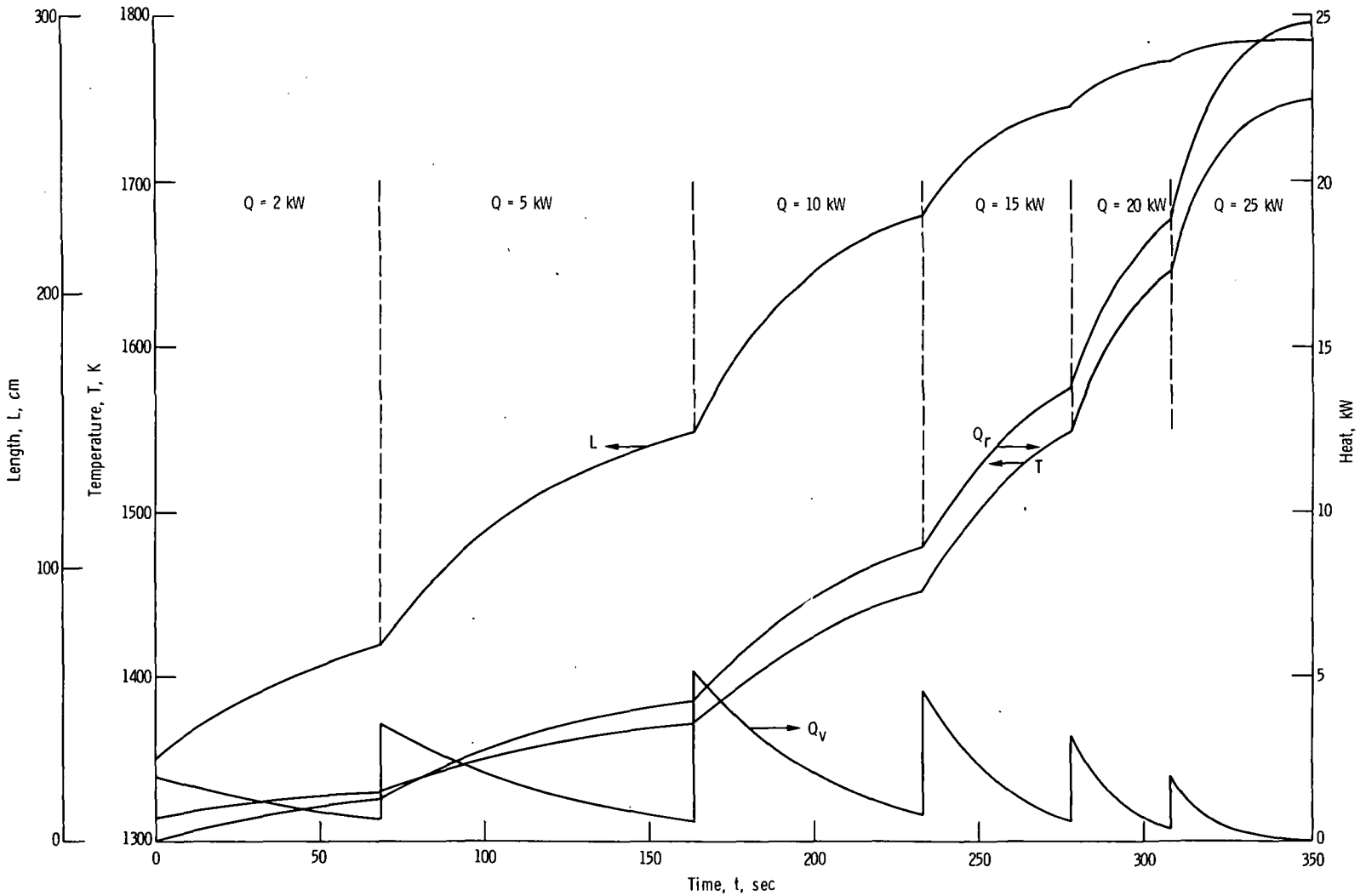

Figure 4. - Startup behavior for an argon-lithium heat pipe with heat input Q increased in steps from 2 to 25 kilowatts. Length of heat pipe, L_p = 300 centimeters; length of evaporator, L_e, 30 centimeters; initial pressure of noncondensible gas, 50 torr; time at which Q is turned on, t_i = -30.4 seconds.

CONCLUSIONS

A two-dimensional diffusion analysis has been used to determine the energy transported by the vapor between the hot and cold zones of a gas-loaded heat pipe. This theory has been combined with a simplified model of the startup process. Numerical results from the combined analysis show that very large diffusion rates occur during startup. Such a result cannot be obtained from a one-dimensional axial diffusion analysis since the radial flow is an essential part of the process.

The numerical results also show that startup is not initiated until the vapor pressure $p_v(T)$ reaches a precise value which is proportional to the initial gas pressure p_i. Hence, startup difficulties can be reduced by selecting a value for p_i such that the pipe will not start until p_v is large enough to support a heat-transfer rate sufficient to overcome the thermal load on the pipe.

Lewis Research Center,
National Aeronautics and Space Administration,
Cleveland, Ohio, May 11, 1973
503-25.

REFERENCES

1. Deverall, J. E.; Kemme, J. E.; and Florschuetz, L. W.: Sonic Limitations and Startup Problems of Heat Pipes. Rep. LA-4518, Los Alamos Scientific Lab., Sept. 1970.

2. Cotter, T. P.: Heat Pipe Startup Dynamics. Proceedings of the Thermionic Conversion Specialist Conference. IEEE, 1967, pp. 344-347.

3. Sockol, Peter M.; and Forman, Ralph: Re-examination of Heat Pipe Startup. Proceedings of the Ninth Thermionic Conversion Specialist Conference. IEEE, 1970, pp. 571-573.

4. Edwards, D. K.; and Marcus, B. D.: Heat and Mass Transfer in the Vicinity of the Vapor-Gas Front in a Gas Loaded Heat Pipe. J. Heat Transfer, vol. 94, no. 2, May 1972, pp. 155-162.

5. Bird, R. Byron; Stewart, Warren E.; and Lightfoot, Edwin N.: Transport Phenomena. John Wiley & Sons, Inc., 1960, p. 502.

6. Abramowitz, Milton; and Stegun, Irene A., eds: Handbook of Mathematical Functions with Formulas, Graphs, and Mathematical Tables. Appl. Math. Ser. 55, National Bureau of Standards, June 1964.

7. Hirschfelder, Joseph O.; Curtiss, Charles F.; and Bird, R. Byron: Molecular Theory of Gases and Liquids. John Wiley & Sons, Inc., 1954, p. 527, 1127.

8. Rothe, Erhard W.; Rol, P. K.; and Bernstein, Richard B.: Interaction Potentials from the Velocity Dependence of Total Atom-Atom Scattering Cross Sections. Phys. Rev., vol. 130, no. 6, June 15, 1963, pp. 2333-2338.

NASA-Langley, 1973 —— 33 E-7416

"The aeronautical and space activities of the United States shall be conducted so as to contribute . . . to the expansion of human knowledge of phenomena in the atmosphere and space. The Administration shall provide for the widest practicable and appropriate dissemination of information concerning its activities and the results thereof."

—NATIONAL AERONAUTICS AND SPACE ACT OF 1958

NASA SCIENTIFIC AND TECHNICAL PUBLICATIONS

TECHNICAL REPORTS: Scientific and technical information considered important, complete, and a lasting contribution to existing knowledge.

TECHNICAL NOTES: Information less broad in scope but nevertheless of importance as a contribution to existing knowledge.

TECHNICAL MEMORANDUMS: Information receiving limited distribution because of preliminary data, security classification, or other reasons. Also includes conference proceedings with either limited or unlimited distribution.

CONTRACTOR REPORTS: Scientific and technical information generated under a NASA contract or grant and considered an important contribution to existing knowledge.

TECHNICAL TRANSLATIONS: Information published in a foreign language considered to merit NASA distribution in English.

SPECIAL PUBLICATIONS: Information derived from or of value to NASA activities. Publications include final reports of major projects, monographs, data compilations, handbooks, sourcebooks, and special bibliographies.

TECHNOLOGY UTILIZATION PUBLICATIONS: Information on technology used by NASA that may be of particular interest in commercial and other non-aerospace applications. Publications include Tech Briefs, Technology Utilization Reports and Technology Surveys.

Details on the availability of these publications may be obtained from:

SCIENTIFIC AND TECHNICAL INFORMATION OFFICE

NATIONAL AERONAUTICS AND SPACE ADMINISTRATION

Washington, D.C. 20546